Nanostructured materials for advanced energy conversion and storage devices

New materials hold the key to fundamental advances in energy conversion and storage, both of which are vital in order to meet the challenge of global warming and the finite nature of fossil fuels. Nanomaterials in particular offer unique properties or combinations of properties as electrodes and electrolytes in a range of energy devices. This review describes some recent developments in the discovery of nanoelectrolytes and nanoelectrodes for lithium batteries, fuel cells and supercapacitors. The advantages and disadvantages of the nanoscale in materials design for such devices are highlighted.

ANTONINO SALVATORE ARICÒ[1], PETER BRUCE[2], BRUNO SCROSATI[3]*, JEAN-MARIE TARASCON[4] AND WALTER VAN SCHALKWIJK[5]

[1]Istituto CNR-ITAE, 98126 S. Lucia, Messina, Italy
[2]School of Chemistry, University of St Andrews, KY16 9ST, Scotland
[3]Dipartimento di Chimica, Università 'La Sapienza', 00186 Rome, Italy
[4]Université de Picardie Jules Verne, LRCS; CNRS UMR-6047, 80039 Amiens, France
[5]EnergyPlex Corporation, 1400 SE 112th Avenue, Suite 210, Bellevue, Washington 98004, USA
*e-mail: scrosati@uniroma1.it

One of the great challenges in the twenty-first century is unquestionably energy storage. In response to the needs of modern society and emerging ecological concerns, it is now essential that new, low-cost and environmentally friendly energy conversion and storage systems are found; hence the rapid development of research in this field. The performance of these devices depends intimately on the properties of their materials. Innovative materials chemistry lies at the heart of the advances that have already been made in energy conversion and storage, for example the introduction of the rechargeable lithium battery. Further breakthroughs in materials, not incremental changes, hold the key to new generations of energy storage and conversion devices.

Nanostructured materials have attracted great interest in recent years because of the unusual mechanical, electrical and optical properties endowed by confining the dimensions of such materials and because of the combination of bulk and surface properties to the overall behaviour. One need only consider the staggering developments in microelectronics to appreciate the potential of materials with reduced dimensions. Nanostructured materials are becoming increasingly important for electrochemical energy storage[1,2]. Here we address this topic. It is important to appreciate the advantages and disadvantages of nanomaterials for energy conversion and storage, as well as how to control their synthesis and properties. This is a sizeable challenge facing those involved in materials research into energy conversion and storage. It is beyond the scope of this review to give an exhaustive summary of the energy storage and conversion devices that may now or in the future benefit from the use of nanoparticles; rather, we shall limit ourselves to the fields of lithium-based batteries, supercapacitors and fuel cells. Furthermore, from now on we shall refer to nanomaterials composed of particles that are of nanometre dimensions as primary nanomaterials, and those for which the particles are typically of micrometre dimensions but internally consist of nanometre-sized regions or domains as secondary nanomaterials.

LITHIUM BATTERIES

Lithium-ion batteries are one of the great successes of modern materials electrochemistry[3]. Their science and technology have been extensively reported in previous reviews[4] and dedicated books[5,6], to which the reader is referred for more details. A lithium-ion battery consists of a lithium-ion intercalation negative electrode (generally graphite), and a lithium-ion intercalation positive electrode (generally the lithium metal oxide, $LiCoO_2$), these being separated by a lithium-ion conducting electrolyte, for example a solution of $LiPF_6$ in ethylene carbonate-diethylcarbonate. Although such batteries are commercially successful, we are reaching the limits in performance using the

current electrode and electrolyte materials. For new generations of rechargeable lithium batteries, not only for applications in consumer electronics but especially for clean energy storage and use in hybrid electric vehicles, further breakthroughs in materials are essential. We must advance the science to advance the technology. When such a situation arises, it is important to open up new avenues. One avenue that is already opening up is that of nanomaterials for lithium-ion batteries

ELECTRODES

There are several potential advantages and disadvantages associated with the development of nanoelectrodes for lithium batteries. Advantages include (i) better accommodation of the strain of lithium insertion/removal, improving cycle life; (ii) new reactions not possible with bulk materials; (iii) higher electrode/electrolyte contact area leading to higher charge/discharge rates; (iv) short path lengths for electronic transport (permitting operation with low electronic conductivity or at higher power); and (v) short path lengths for Li^+ transport (permitting operation with low Li^+ conductivity or higher power). Disadvantages include (i) an increase in undesirable electrode/electrolyte reactions due to high surface area, leading to self-discharge, poor cycling and calendar life; (ii) inferior packing of particles leading to lower volumetric energy densities unless special compaction methods are developed; and (iii) potentially more complex synthesis.

With these advantages and disadvantages in mind, efforts have been devoted to exploring negative and, more recently, positive nanoelectrode materials.

ANODES

Metals that store lithium are among the most appealing and competitive candidates for new types of anodes (negative electrodes) in lithium-ion batteries. Indeed, a number of metals and semiconductors, for example aluminium, tin and silicon, react with lithium to form alloys by electrochemical processes that are partially reversible and of low voltage (relative to lithium), involve a large number of atoms per formula unit, and in particular provide a specific capacity much larger than that offered by conventional graphite[7,8]. For example, the lithium–silicon alloy has, in its fully lithiated composition, $Li_{4.4}Si$, a theoretical specific capacity of 4,200 mA h g^{-1} compared with 3,600 mA h g^{-1} for metallic lithium and 372 mA h g^{-1} for graphite. Unfortunately, the accommodation of so much lithium is accompanied by enormous volume changes in the host metal plus phase transitions. The mechanical strain generated during the alloying/de-alloying processes leads to cracking and crumbling of the metal electrode and a marked loss of capacity to store charge, in the course of a few cycles[8,9].

Although these structural changes are common to alloying reactions, there have been attempts to limit their side effects on the electrode integrity. Among them, the active/inactive nanocomposite concept

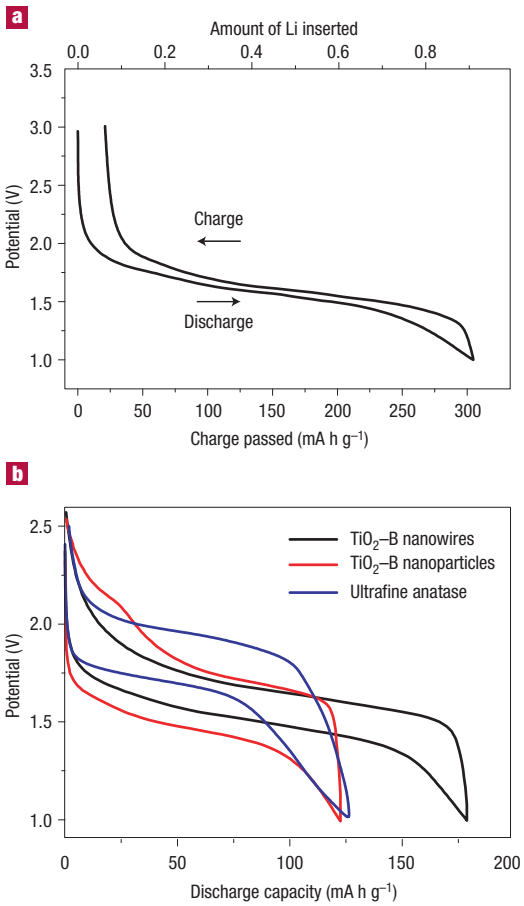

Figure 1 Charge–discharge curves for nanostructured anode materials. **a**, Charge–discharge curves for Li_xTiO_2-B nanowires (rate of 10 mA g^{-1}). **b**, Comparison of cycling behaviour for TiO_2-B nanowires, TiO_2-B nanoparticles and nanoparticulate anatase, all at 200 mA g^{-1}.

represents one attractive route. Several authors[7–9] have discussed this approach, which involves intimately mixing two materials, one reacting with lithium wheras the other acts as an inactive confining buffer. Within this composite, the use of nano-size metallic clusters as lithium hosts considerably suppresses the associated strains, and therefore improves the reversibility of the alloying reaction. By applying this concept through different systems such as SnO-based glasses[10], or composites such as Sn–Fe–C (ref. 11), Sn–Mn–C (ref. 12) or Si–C (refs 13–15), several authors have demonstrated that these electrodes show a considerable improvement in their cycling response in lithium cells. The Si–C nanocomposites have attracted considerable interest because they show capacity as high as 1,000 mA h g^{-1} for more than 100 cycles[15]. Some of these improvements may arise because the materials avoid cracking, thus maintaining better conduction pathways, or because they incorporate conductive additives such as carbon. Undoubtedly alloy performance can also benefit from nanostructuring. For instance, thin amorphous silicon films deposited on a specially roughened copper foil surface by a sputtering process were shown[16] to have close to 100% reversibility at capacities larger than 3,000 mA h g^{-1}. An excellent capacity retention was also noted for silicon electrodes prepared with a nanopillar surface morphology[17] because size confinement alters particle deformation and reduces fracturing.

Table 1 The Gibbs free energy change ΔG of conversion reactions. Values are obtained using thermodynamic data given in the literature[22] for various compounds together with the corresponding electromotive force (e.m.f.) values E, as deduced from the well-known $\Delta G = -nEF$ where F is Faraday's constant.

Compound		ΔG (kg mol^{-1})	E(V) = E_{eq} (volts vs Li$^+$/Li^o)
$CoS_{0.89}$	(+2)	–265.5	1.73
CoO	(+2)	–347.0	1.79
$CoCl_2$	(+2)	–499.0	2.59
CoF_2	(+2)	–528.2	2.74
CoF_3	(+3)	–1,023.4	3.54

Perhaps the greatest disadvantage of primary nanoparticles is the possibility of significant side-reactions with the electrolyte, leading to safety concerns (one of the most critical issues for lithium batteries) and poor calendar life. But if the materials fall within the stability window of the electrolyte or at least limit the formation of the solid–electrolyte interface (SEI) layer, then the many advantages of nanoparticles may more easily be exploited. Such an example is $Li_{4+x}Ti_5O_{12}$ ($0 < x < 3$, 160 mA h g^{-1}, 1.6 V versus Li$^+$(1M)/Li). No evidence has been reported for a significant surface layer formation (presumably because the potential is sufficiently high compared with lithium), and this material can be used as a nanoparticulate anode with high rate capability and good capacity retention. Controlling the nanoparticle shape as well as size can offer advantages. This is illustrated by recent results on TiO_2-B nanotubes or wires (B designates the form of TiO_2 and not boron). Such materials may be synthesized by a simple aqueous route and in high yield, with diameters in the range of 40–60 nm and lengths up to several micrometres. The TiO_2-B polymorph is an excellent intercalation host for Li, accommodating up to $Li_{0.91}TiO_2$-B (305 mA h g^{-1}) at 1.5–1.6 V vs Li$^+$(1M)/Li and with excellent capacity retention on cycling (Fig. 1). Interestingly, the rate capability is better than the same phase prepared as nanoparticles of dimension similar to the diameter of the nanowires[18] (Fig. 1). These TiO_2-B electrodes are not the only nanotube/wire electrodes. Unsurprisingly, carbon nanotubes have been explored as anodes. Whether the cost of their synthesis is viable remains an open question.

Nanomaterials consisting of nanoparticles or nanoarchitectured materials, as described so far in this review, are not always easy to make because of difficulties in controlling the size and size distribution of the particles or clusters. The potential disadvantage of a high external surface area, leading to excessive side reactions with the electrolyte and hence capacity losses or poor calendar life, has already been mentioned. Such problems may be addressed with internally nanostructured materials (secondary nanomaterials as defined), where the particles are significantly larger than the nanodomains. As well as reducing side reactions with the electrolyte, this can have the advantage of ensuring higher volumetric energy densities. Of course, as described below, they are not a panacea.

A group of internally nanostructured anodes based on transition metal oxides has recently been described. The full electrochemical reduction of oxides such as CoO, CuO, NiO, Co_3O_4 and MnO versus lithium, involving two or more electrons per 3*d*-metal, was shown to lead to composite materials consisting of nanometre-scale metallic clusters dispersed in an amorphous Li_2O matrix[19]. Owing to the nanocomposite nature of these electrodes, the reactions, termed 'conversion reactions', are highly reversible, providing large capacities that can be maintained for hundreds of cycles. The prevailing view had been that reversible lithium reaction could occur only in the presence of crystal structures with channels able to transport Li$^+$. The new results, in stark contrast, turn out not to be specific to oxides but can be extended to sulphides, nitrides or fluorides[20]. These findings help to explain the previously reported unusual reactivity of complex oxides including RVO_4 (R = In, Fe) or A_xMoO_3 towards lithium[21,22].

Such conversion reactions offer numerous opportunities to 'tune' the voltage and capacity of the cell[19] owing to the fact that the cell potential is directly linked to the strength of the M–X bonding. Weaker M–X bonding gives larger potentials. The capacity is directly linked to the metal oxidation state, with the highest capacity associated with the highest oxidation states. Thus, by selecting the nature of M and its oxidation state, as well as the nature of the anion, one can obtain reactions with a specific potential within the range 0 to 3.5 V (Table 1), and based on low-cost elements such as Mn or Fe. Fluorides generally yield higher potentials than oxides, sulphides and nitrides.

However, such excitement needs to be tempered because ensuring rapid and reversible nanocomposite reactions is not an easy task. The future of such conversion reactions in real-life applications lies in mastering their kinetics (for example, the chemical diffusion of lithium into the matrix). Great progress has already been achieved with oxides, especially metallic RuO_2, which was shown[23] to display a 100% reversible conversion process involving 4e$^-$, and some early but encouraging results have been reported with

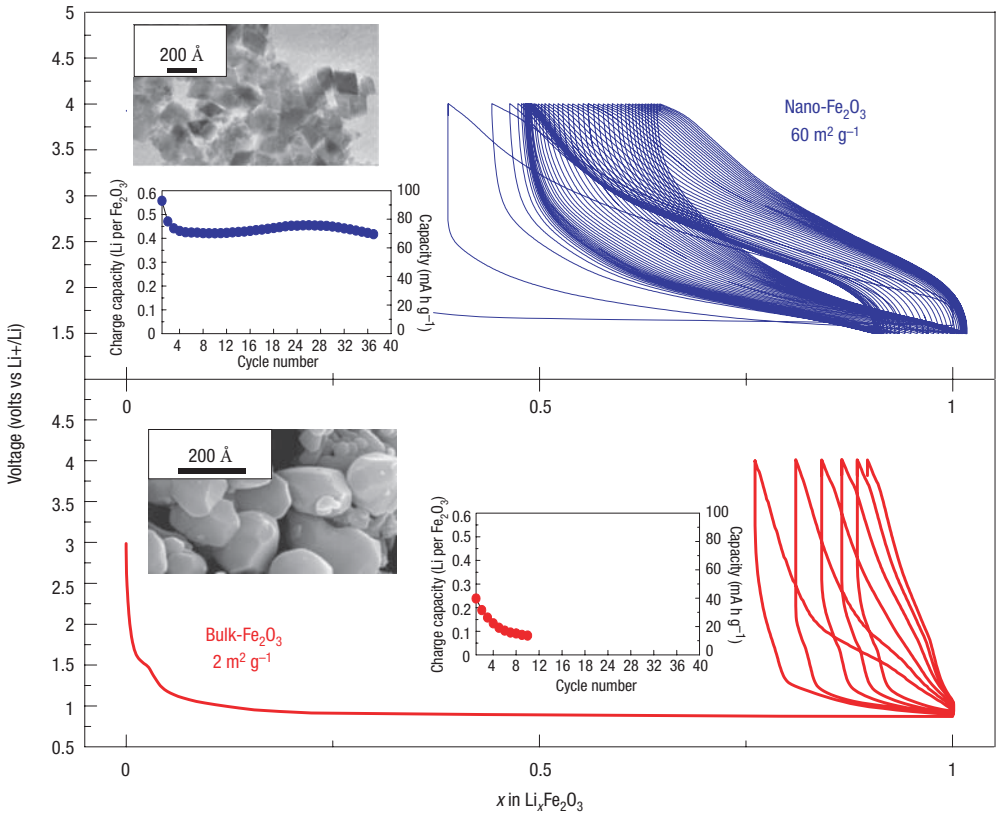

Figure 2 Electrochemical behaviour of bulk and nanostructured α-Fe_2O_3 with voltage–composition curves. The capacity retention and scanning electron micrographs of both samples are shown in the insets.

fluorides[24–26]; but a great deal remains to be done in this area. A further hint that working at the nanoscale may radically change chemical/electrochemical reaction paths of inorganic materials comes from recent studies carried out on the reactivity of macroscopic versus nanoscale haematite (α-Fe_2O_3) particles with Li. With nanometre-scale haematite particles (20 nm), reversible insertion of 0.6 Li per Fe_2O_3 is possible through a single-phase process, whereas large haematite particles (1 to 2 μm) undergo an irreversible phase transformation as soon as ~0.05 Li per Fe_2O_3 are reacted (see Fig. 2)[27]. In this respect, many materials, previously rejected because they did not fulfil the criteria as classical intercalation hosts for lithium, are now worth reconsideration.

CATHODES

This area is much less developed than the nanoanodes. The use of nanoparticulate forms (primary nanomaterials) of the classical cathode materials such as $LiCoO_2$, $LiNiO_2$ or their solid solutions can lead to greater reaction with the electrolyte, and ultimately more safety problems, especially at high temperatures, than the use of such materials in the micrometre range. In the case of Li–Mn–O cathodes such as $LiMn_2O_4$, the use of small particles increases undesirable dissolution of Mn. Coating the particles with a stabilizing surface layer may help to alleviate such problems but can reduce the rate of intercalation, reducing the advantage of the small particles.

A related approach to the formation of silicon nanopillars has been taken for cathode materials. By using a template, for example, porous alumina or a porous polymer, nanopillars of V_2O_5 or $LiMn_2O_4$ have been grown on a metal substrate[28]. These microfabricated electrode structures have the advantages of the Si example, accommodating volume changes and supporting high rates, although in the case of the manganese oxide, accelerated dissolution is expected. Nanotubes of VO_x have also been prepared and investigated as cathodes[29].

Tuning the electrode material morphology or texture to obtain porous and high-surface-area electrodes constitutes another route to enhance electrode capacities[30]. For V_2O_5, aerogels (disordered mesoporous materials with a high pore volume) were recently reported to have electroactive capacities greater than polycrystalline non-porous V_2O_5 powders[31]. Such aerogels present a large surface area to the electrolyte, and can support high rates, although cyclability can be a problem because of structural changes or very reactive surface groups.

Interesting developments in secondary particle cathodes for lithium batteries have taken place in parallel with the work on secondary particle anodes. By retaining large particles, there is less dissolution than with primary nanoparticulate materials, and high volumetric densities are retained. Conventional wisdom stated that to sustain rapid and reversible electrode reactions in rechargeable lithium batteries, intercalation compounds must be used as the electrodes, and that the intercalation process had to be single-phase, that is, a continuous solid solution on

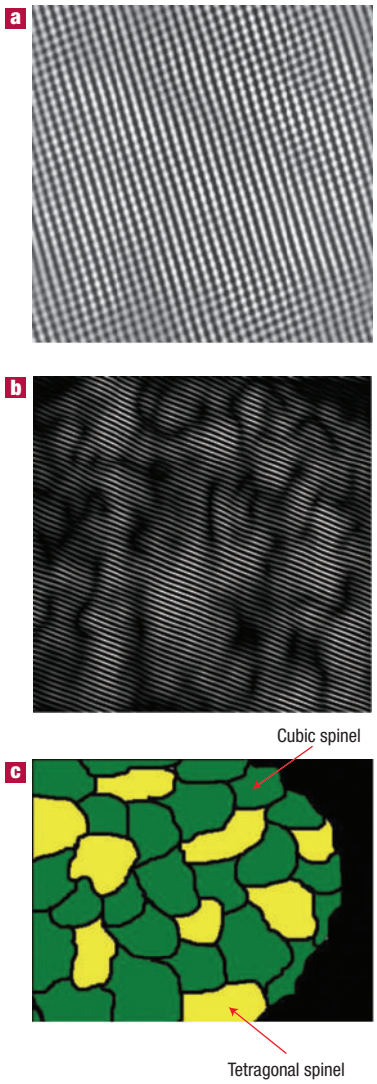

Figure 3 Transmission electron micrographs of regular and nanostructured spinel. a, Regular $Li_xMn_{2-y}O_4$ spinel. **b**, $Li_xMn_{2-y}O_4$ spinel obtained on cycling layered (O3) $Li_xMn_{1-y}O_2$. The Fourier-filtered image (**b**) highlights the nanodomain structure of average dimensions 50–70 Å. **c**, A schematic representation of the nanodomain structure of $Li_xMn_{2-y}O_4$ spinel derived from layered $Li_xMn_{1-y}O_2$, showing cubic and tetragonal nanodomains.

intercalation. However, there are now many examples where lithium intercalation is facile despite undergoing phase transitions, including $LiCoO_2$ and $Li_4Ti_5O_{12}$, especially if there is a strong structural similarity between the end phases (for example, only differences in Li ordering). Such two-phase intercalation reactions are far from being universally reversible. A classic example[32] is the intercalation cathode $Li_xMn_2O_4$, $0 < x < 2$. Cycling is usually confined to the range $0 < x < 1$ to avoid the transformation of cubic $LiMn_2O_4$ to tetragonal $Li_2Mn_2O_4$, which leads to a marked loss of capacity (ability to cycle lithium) because of the 13% anisotropy in the lattice parameters on formation of the tetragonal phase. Layered $LiMnO_2$ with the α-$NaFeO_2$ structure transforms into spinel on cycling but may be cycled with >99.9% capacity retention, despite undergoing the same cubic–tetragonal transformation[33]. The reason is clearly not suppression of the Jahn–Teller driven cubic–tetragonal distortion (something that has been attempted many times with limited success). Instead, the system accommodates the strain associated with the transformation by developing a nanostructure within the micrometre-sized particles (Fig. 3). The nanodomains of spinel switch between cubic and tetragonal structures, with the strain being accommodated by slippage at the domain wall boundaries[34,35]. The nanodomains form during the layered-to-spinel transformation. Subsequently it has been shown that such a nanostructure can be induced in normal spinel by grinding, with a similar enhancement in cyclability[36]. Interestingly, the layered-to-spinel transformation is very easy, helping to mitigate any ill effects the transformation itself may have on cyclability[37].

A further, somewhat different, example of the benefits of nanoelectrodes within the field of batteries is the optimization of the environmentally benign and low-cost phospho-olivine $LiFePO_4$ phase[38] that displays a theoretical capacity of 170 mA h g^{-1}, as compared with 140 mA h g^{-1} for the $LiCoO_2$ electrode used at present ($LiFePO_4$ operates at a lower voltage). But the insulating character of the olivine means that in practice one could not obtain the full capacity of the material because, as the electrochemical reaction proceeds, 'electronically' isolated areas remain inactive in the bulk electrode. As a result, this material was largely ignored until it was prepared in the form of carbon-coated nanoparticles (Fig. 4) through various chemical and physical means[39–41]. This simultaneously reduces the distance for Li^+ transport, and increases the electronic contact between the particles. Procedures of this kind have led to a greatly improved electrochemical response, and the full capacity of the material is now accessible even under prolonged cycling[39] (see also Fig. 4). This example serves to illustrate some of the advantages of nanoelectrode materials listed at the beginning of this section, and to demonstrate that the search for new electroactive materials is now wider than ever because such materials do not require a particularly high electronic conductivity, nor a high diffusion coefficient for lithium, as had been believed for the past 20 years.

ELECTROLYTES

Progress in lithium batteries relies as much on improvements in the electrolyte as it does on the electrodes. Solid polymer electrolytes represent the ultimate in terms of desirable properties for batteries because they can offer an all-solid-state construction, simplicity of manufacture, a wide variety of shapes and sizes, and a higher energy density (because the constituents of the cell may be more tightly wound). No corrosive or explosive liquids can leak out, and internal short-circuits are less likely, hence greater safety. The most desirable polymer electrolytes are those formed by solvent-free membranes, for example poly(ethylene oxide), PEO, and a lithium salt, LiX, for example $LiPF_6$ or $LiCF_3SO_3$ (ref. 42). The poor ionic conductivity of these materials at room temperature has prevented them from realizing their otherwise high promise. Dispersing nanoscale inorganic fillers in solvent-free, polyether-based electrolytes increases the

conductivity several-fold[43–45]. The improvement of the electrolyte transport properties may be explained on the basis of the heterogeneous doping model developed by Maier[46]. Accordingly, nanocomposites can be defined as the distribution of a second (or even third) phase, with particles of nanometric dimension in a matrix that can be amorphous or crystalline. Thus the increase in conductivity may be associated with Lewis acid–base interactions between the surface states of the ceramic nanoparticle with both the polymer chains and the anion of the lithium salt[47]. As in the electrode case, there are of course pros and cons in this particular approach. Indeed, other avenues are being explored to achieve high-conductivity polymer electrolytes. Relevant in this respect are the polymer-in-salt nanostructures[48] and the role of ionic liquids[49].

For 30 years it has been accepted that ionic conductivity in polymer electrolytes occurred exclusively in the amorphous phase, above the glass transition temperature T_g. Crystalline polymer electrolytes were considered to be insulators. But recent studies have shown that this is not the case: the 6:1 crystalline complexes PEO_6:$LiXF_6$; X = P, As, Sb demonstrate ionic conductivity[50,51]. The Li^+ ions reside in tunnels formed by the polymer chains (Fig. 5). Significant increases in ionic conductivity in the crystalline 6:1 complexes are observed on reducing the chain length from 3,000 to 1,000: that is, in the nanometre range[52]. It is evident that in electrolytes, just as in the electrodes described above, control of dimensions on the nanoscale has a profound influence on performance[52]. Crystalline polymer electrolytes represent a radically different type of ionic conductivity in polymers, and illustrate the importance of seeking new scientific directions. The present materials do not support ionic conductivities that are sufficient for applications, but they do offer a fresh approach with much scope for further advances. Recently it has been shown that the conductivity of the crystalline polymer electrolytes may be raised by two orders of magnitude by partial replacement of the XF_6 ions with other mono or divalent anions (ref. 53, and P. G. Bruce, personal communication). Chemical compatibility with selected electrode materials has yet to be evaluated.

SUPERCAPACITORS

Supercapacitors are of key importance in supporting the voltage of a system during increased loads in everything from portable equipment to electric vehicles[54–56]. These devices occupy the area in the Ragone plot (that is, the plot of volumetric against gravimetric energy density) between batteries and dielectric capacitors. Supercapacitors are similar to batteries in design and manufacture (two electrodes, separator and electrolyte), but are designed for high power and long cycle life (>100 times battery life), but at the expense of energy density.

There are two general categories of electrochemical supercapacitors: electric double-layer capacitors (EDLC) and redox supercapacitors. In contrast to batteries, where the cycle life is limited because of the repeated contraction and expansion of the electrode on cycling, EDLC lifetime is in principle infinite, as it operates solely on electrostatic surface-charge accumulation. For redox supercapacitors, some fast faradic charge transfer takes place as in a battery. This gives rise to a large pseudo-capacitance.

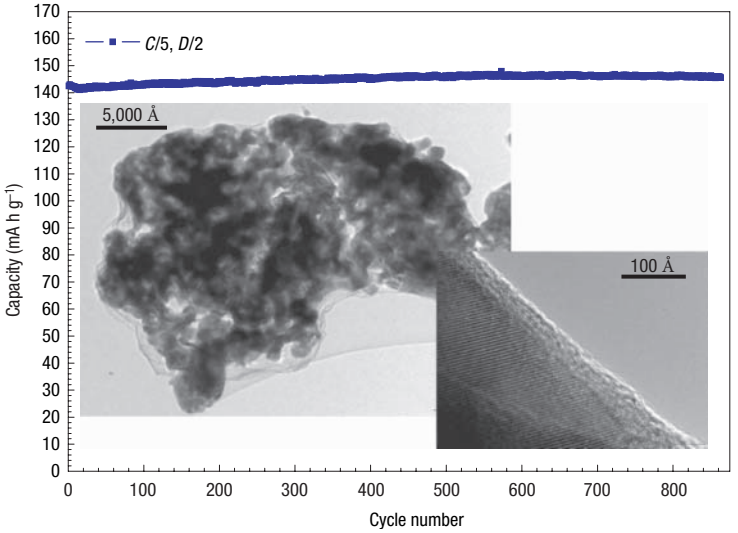

Figure 4 Capacity against cycling number for a lithium coin cell. The experiments used a 1-cm^2 disc of Bellcore-type plastic laminate made out 4.480 mg of pure $LiFePO_4$ coated with 5% C *in situ*. The overall plastic composition was 69% $LiFePO_4$, 11% C total and 20% Kynar. The cell was cycled at *C*/5 (0.160 mA cm^{-2}), *D*/2 (–0.400 mA cm^{-2}) between 2 and 4.5 V at room temperature. Here, *D* is discharge rate, *C* is charge rate. Left inset: enlarged transmission electron micrograph of the $LiFePO_4$ particles used, coated with carbon. The coating used a homemade recipe[103]. This image was recorded with a TECNAI F20 scanning TEM. The quality of the coating — that is, the interface between crystallized $LiFePO_4$ and amorphous carbon — is nicely observed in the high-resolution electron micrograph in the right inset (taken with the same microscope). Courtesy of C. Wurm and C. Masquelier, LRCS Amiens.

Progress in supercapacitor technology can benefit by moving from conventional to nanostructured electrodes. In the case of supercapacitors, the electrode requirements are less demanding than in batteries, at least in terms of electrode compaction, because power prevails over energy density. Thus, the benefits of nanopowders with their high surface area (primary nanoparticles) are potentially more important, hence the staggering interest in nanopowders and their rapid uptake for supercapacitor-based storage sources.

Recent trends in supercapacitors involve the development of high-surface-area activated carbon electrodes to optimize the performance in terms of capacitance and overall conductivity. Attention has been focused on nanostructured carbons, such as aerogels[57], nanotubes[58] and nanotemplates[59]. The advantages of carbon aerogels lie mainly in their low ionic and electronic charging resistance and in their potential use as binderless electrodes. Replacing the standard carbon fibre with carbon aerogel electrodes improves capacitance and cyclability. Because of their unique architecture, carbon nanotubes are now intensively studied as new electrode materials for supercapacitor structures although, as for batteries, cost may be an issue. A critical aspect in nanotechnology for supercapacitors is to reach a compromise between specific surface area (to ensure high capacitance) and pore-size distribution (to permit easy access for the electrolyte).

Nanostructured materials have led to the development of new supercapacitor technologies. Capitalizing on the benefits of nanomaterial electrodes, Telcordia's researchers have, by means of the so-called hybrid supercapacitors (HSCs), proposed a new approach to energy storage[60]. HSCs use one capacitive carbon electrode similar to that of a carbon EDLC; however, the complementary negative electrode consists of a nanostructured lithium

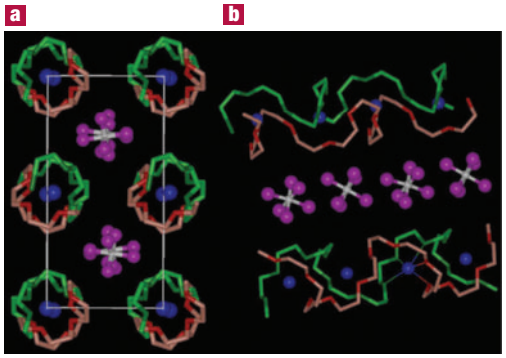

Figure 5 The structures of PEO_6:$LiAsF_6$. **a**, View of the structure along *a* showing rows of Li^+ ions perpendicular to the page. **b**, View of the structure showing the relative position of the chains and its conformation (hydrogens not shown). Thin lines indicate coordination around the Li^+ cation. Blue spheres, lithium; white spheres, arsenic; magenta, fluorine; green, carbon; red, oxygen.

titanate compound that undergoes a reversible faradic intercalation reaction[61]. The key innovation lies in the use of a nanostructured $Li_4Ti_5O_{12}$ as the negative electrode, resulting in no degradation in performance from charge/discharge-induced strain. Here is a nanomaterial that is being explored for capacitor and battery use because of its excellent cyclability, rate capability and safety. Its use in the hybrid supercapacitor results in a device with cycle life comparable to that of supercapacitors, freeing designers from the lifespan limitations generally associated with batteries. Figure 6 shows some features of these new types of capacitors. Besides $Li_4Ti_5O_{12}$, other nanostructured oxide materials can be engineered so as to obtain hybrid devices operating over a wide range of voltages. Inorganic nanotubes or nanowires may offer an alternative to nanoparticulate $Li_4Ti_5O_{12}$, for example the Li_xTiO_2-B nanowires described in the section on lithium batteries. One can therefore envisage a supercapacitor composed of a carbon nanotube as the positive electrode and an inorganic nanotube capable of lithium intercalation (for example Li_xTiO_2-B) as the negative electrode.

Fabricating nanopillared electrodes by growing the materials on a substrate was described in the context of lithium batteries. However, a related approach where materials are electro-synthesized in the presence of an electrolyte, which is also a liquid-crystal template, has been used to form nanoarchitectured electrodes, for example Ni or NiOOH, for possible use in supercapacitors[61].

FUEL CELLS

Fuel cell technologies are now approaching commercialization, especially in the fields of portable power sources — distributed and remote generation of electrical energy[62]. Already, nanostructured materials are having an impact on processing methods in the development of low-temperature fuel cells ($T < 200$ °C), the dispersion of precious metal catalysts, the development and dispersion of non-precious catalysts, fuel reformation and hydrogen storage, as well as the fabrication of membrane-electrode assemblies (MEA). Polymer electrolyte membrane fuel cells (PEMFCs) have recently gained momentum for application in transportation and as small portable power sources; whereas phosphoric acid fuel cells (PAFCS), solid oxide fuel cells (SOFCs) and molten carbonates fuel cells (MCFCs) still offer advantages for stationary applications, and especially for co-generation[62]. Platinum-based catalysts are the most active materials for low-temperature fuel cells fed with hydrogen, reformate or methanol[62]. To reduce the costs, the platinum loading must be decreased (while maintaining or improving MEA performance), and continuous processes for fabricating MEAs in high volume must be developed. A few routes are being actively investigated to improve the electrocatalytic activity of Pt-based catalysts. They consist mainly of alloying Pt with transition metals or tailoring the Pt particle size.

The oxygen reduction reaction (ORR) limits the performance of low-temperature fuel cells. One of the present approaches in order to increase the catalyst dispersion involves the deposition of Pt nanoparticles on a carbon black support. Kinoshita *et al.* observed that the mass activity and specific activity for oxygen electro-reduction in acid electrolytes varies with the Pt particle size according to the relative fraction of Pt surface atoms on the (111) and (100) faces[63] (Fig. 7). The mass-averaged distribution of the surface atoms on the (111) and (100) planes passes through a maximum (~3 nm) whereas the total fraction of surface atoms at the edge and corner sites decreases rapidly with an increase of the particle size. On the other hand, the surface-averaged distribution for the (111) and (100) planes shows a rapid increase with the particle size, which accounts for the increase of the experimentally determined specific activity with the particle size (Fig. 7). A dual-site reaction is assumed as the rate-determining step:

$$O_2 + Pt \rightarrow Pt\text{–}O_2$$

$$Pt\text{-}O_2 + H^+ + e^- \rightarrow Pt\text{-}HO_2$$

$$Pt\text{–}HO_2 + Pt \rightarrow Pt\text{–}OH + Pt\text{–}O \text{ (r.d.s.)}$$

$$Pt\text{–}OH + Pt\text{–}O + 3H^+ + 3e^- \rightarrow 2Pt + 2H_2O$$

This mechanism accounts for the role of dual sites of proper orientation[63].

Alloying Pt with transition metals also enhances the electrocatalysis of O_2 reduction. In low-temperature fuel cells, Pt–Fe, Pt–Cr and Pt–Cr–Co alloy electrocatalysts were observed[62,64,65] to have high specific activities for oxygen reduction as compared with that on platinum. This enhancement in electrocatalytic activity has been ascribed to several factors such as interatomic spacing, preferred orientation or electronic interactions. The state of the art Pt–Co–Cr electrocatalysts have a particle size of 6 nm (ref. 65).

Both CO_2 and CO are present in hydrogen streams obtained from reforming. These molecules are known to adsorb on the Pt surface under reducing potentials. Adsorbed CO-like species are also formed on Pt-based anode catalysts in direct methanol fuel cells (DMFCs). Such a poisoning of the Pt surface reduces the electrical efficiency and the power density of the fuel cell[66]. The electrocatalytic activity of Pt against, for example, CO_2/CO poisoning is known to be promoted by the presence of a second metal[64,65,67], such as Ru, Sn or Mo. The mechanism by which such synergistic promotion of the H_2/CO and methanol

oxidation reactions is brought about has been much studied and is still debated. Nevertheless, it turns out that the best performance is obtained from Pt–Ru electrocatalysts with mean particle size 2–3 nm. As in the case of oxygen reduction, the particle size is important for structure-sensitive reactions such as CH_3OH and CO electro-oxidation. The catalytic activity of Pt–Ru surfaces is maximized for the (111) crystallographic plane[68]. According to the bifunctional theory, the role of Ru in these processes is to promote water discharge and removal of strongly adsorbed CO species at low potentials through the following reaction mechanism[66–68]:

$$Ru + H_2O \rightarrow Ru{-}OH + H^+ + 1e^-$$

$$Ru{-}OH + Pt{-}CO \rightarrow Ru + Pt + CO_2 + H^+ + 1e^-$$

A change in the CO binding strength to the surface induced by Ru through a ligand effect on Pt has been reported[66,67].

The synthesis of Pt-based electro-catalysts, either unsupported or supported on high-surface-area carbon, is generally carried out by various colloidal preparation routes. A method recently developed by Bönnemann and co-workers[67] allows fine-tuning of the particle size for the bimetallic Pt–Ru system.

Recent developments in the field of CO-tolerant catalysts include the synthesis of new nanostructures by spontaneous deposition of Pt sub-monolayers on carbon-supported Ru nanoparticles[68,69]. This also seems to be an efficient approach to reduce the Pt loading. Further advances concern a better understanding of the surface chemistry in electrocatalyst nanoparticles and the effects of strong metal–support interactions that influence both the dispersion and electronic nature of platinum sites.

An alternative approach, avoiding the use of carbon blacks, is the fabrication of porous silicon catalyst support structures with a 5-μm pore diameter and a thickness of about 500 μm. These structures have high surface areas, and they are of interest for miniature PEM fuel cells[70]. A finely dispersed, uniform distribution of nanometre-scale catalyst particles deposited on the walls of the silicon pores creates, in contact with the ionomer, an efficient three-phase reaction zone capable of high power generation in DMFCs[70].

As an alternative to platinum, organic transition metal complexes — for example, iron or cobalt organic macrocycles from the families of phenylporphyrins[71] and nanocrystalline transition metal chalcogenides[72] — are being investigated for oxygen reduction, especially in relation to their high selectivity towards the ORR and tolerance to methanol cross-over in DMFCs. The metal–organic macrocycle is supported on high-surface-area carbon, and treated at high temperatures (from 500 to 800 °C) to form a nanostructured compound that possesses a specific geometrical arrangement of atoms. These materials show suitable electrocatalytic activity, even if smaller than that of Pt, without any degradation in performance[71].

As for batteries, the electrolyte is a key component of the fuel cell assembly. Perfluorosulphonic polymer electrolyte membranes (for example Nafion™) are currently used in H_2/air or methanol/air fuel cells because of their excellent conductivity and electrochemical stability[62]. Unfortunately, they suffer from several drawbacks such as methanol cross-over and membrane dehydration. The latter severely hinders the fuel cell operation above 100 °C, which is a prerequisite for the suitable oxidation of small organic molecules involving formation of strongly adsorbed reaction intermediates such as CO-like species[63,66,67]. Alternative membranes based on poly(arylene ether sulphone)[73], sulphonated poly(ether ketone)[74] or block co-polymer ion-channel-forming materials as well as acid-doped polyacrylamid and polybenzoimidazole have been suggested[75–77]. Various relationships between membrane nanostructure and transport characteristics, including conductivity, diffusion, permeation and electro-osmotic drag, have been observed[78]. Interestingly, the presence of less-connected hydrophilic channels and larger separation of sulphonic groups in sulphonated poly(ether ketone) than in Nafion reduces water permeation and electro-osmotic drag whilst maintaining high protonic conductivity[78]. Furthermore, an improvement in thermal and mechanical stability has been shown in nano-separated acid–base polymer blends obtained by combining polymeric N-bases and polymeric sulphonic acids[74]. Considerable efforts have been addressed in the last decade to the development of composite membranes. These include ionomeric membranes modified by dispersing inside their polymeric matrix insoluble acids, oxides, zirconium phosphate and so on; other examples are ionomers or inorganic solid acids with high proton conductivity, embedded in porous non-proton-conducting polymers[75]. Recently, Alberti and Casciola[75] prepared nanocomposite electrolytes by *in situ* formation of insoluble layered Zr phosphonates in ionomeric membranes. Such compounds, for example $Zr(O_3P{-}OH)(O_3P{-}C_6H_4{-}SO_3H)$, show conductivities much higher than the Zr phosphates and comparable to Nafion. In an attempt to reduce

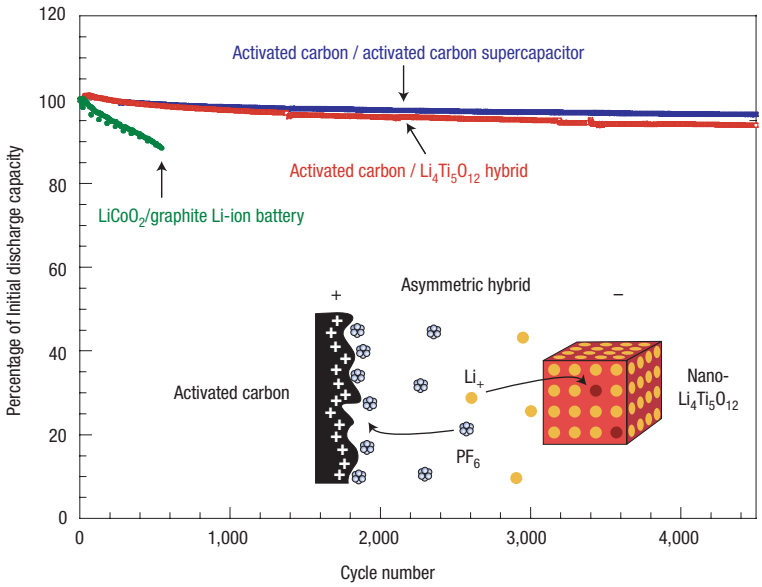

Figure 6 Cycling performance of the new asymmetric hybrid C/nano-$Li_4Ti_5O_{12}$ supercapacitor. Shown for comparison are results for a classical C/C supercapacitor and a commercial lithium-ion battery. The basic concept of this new type of supercapacitor is shown as an inset.

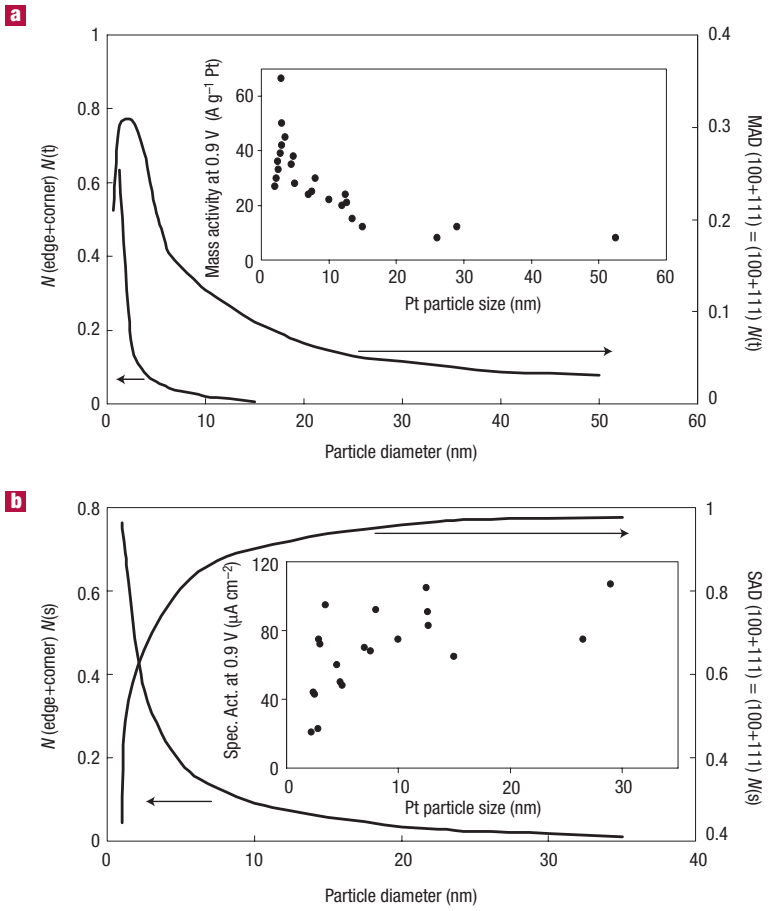

Figure 7 Calculated mass-averaged (a) and surface-averaged distributions (b) as a function of particle size in Pt particles with cubo-octahedral geometry. The values of *N*(t) and *N*(s) indicate the total number of atoms and the number of atoms on the surface respectively. The variation with particle size of mass activity (**a**) and specific activity (**b**) for oxygen reduction in acid electrolyte is shown in the insets[63].

the drawbacks of perfluorosulphonic membranes, nanoceramic fillers have been included in the polymer electrolyte network. Stonehart, Watanabe and co-workers[79] have successfully reduced the humidification constraints in PEMFCs by the inclusion of small amounts of SiO_2 and Pt/TiO_2 (~7 nm) nanoparticles to retain the electrochemically produced water inside the membrane. Similarly modified membranes, containing nanocrystalline ceramic oxide filler, have been demonstrated[80] to operate up to 150 °C. Although it has been hypothesized[75–77] that the inorganic filler induces structural changes in the polymer matrix, the water-retention mechanism appears more likely to be favoured by the presence of acidic functional groups on the surface of nanoparticle fillers[81]. At present, there are no indications that the transport properties are significantly affected by the filler[82]. However, the greater water retention capability of the composite membrane at high temperatures (130 °C–150 °C) and under low humidity[81] should promote the 'vehicular mechanism' of proton conduction as occurs at lower temperatures[83]. Investigation of the lifetime behaviour of composite membranes, under low humidity, needs to be carried out in the next few years to assess these electrolyte materials.

Within the PEMFCs, the Pt/C catalyst is intimately mixed with the electrolyte ionomer to form a composite catalyst layer extending the three-phase reaction zone. This is similar to the composite cathode approach in lithium-ion batteries where the electrode consists of two interpenetrating networks for electron and ion conduction; the benefit of this approach is an enhancement of the interfacial region between catalyst particles and ionomer[62,84]. A reduction in the Pt content to significantly less than 0.5 mg cm^{-2} without degrading the cell performance and life-time has been demonstrated[62,84]. Following this general concept, durable multi-level MEAs are being developed (3M Corporation) using high-speed precision coating technologies and an automated assembly process[85]. Part of the MEA is a nanostructured thin-film catalyst based on platinum-coated nano-whiskers. The approach uses highly oriented, high-aspect-ratio single-crystalline whiskers of an organic pigment material. Typically there are 3×10^9 to 5×10^9 whiskers cm^{-2}. This support permits suitable specific activity of the applied catalysts and aids processing and manufacturing. However, the electrocatalytic activities so obtained are comparable to catalyst–ionomer inks. Platinum-coated nano-whiskers and a cross-section of the MEA are shown in Fig. 8.

The trend towards nanomaterials is not limited to low-temperature fuel cells. Nanostructured electro-ceramic materials are increasingly used in intermediate-temperature solid oxide fuel cells (IT-SOFCs). Although one may start with nanosized particles in the fabrication of SOFCs materials, these are often modified by the temperatures required for cell fabrication (>1,000 °C), thus forming microstructured components with electro-catalytic and ion-conduction properties different from the typical polycrystalline materials[86]. Nanosized YSZ (8% Y_2O_3–ZrO_2) and ceria-based (CGO, SDC, YDC) powders permit a reduction of the firing temperature during the membrane-forming step in the cell fabrication procedure, because their sintering properties differ from those of polycrystalline powders[87]. Furthermore, nanocrystalline ceria, which is characterized by mixed electronic–ionic conduction properties, promotes the charge transfer reactions at the electrode–electrolyte interface[87].

Ionic charge carriers in electro-ceramic materials originate from point defects. In nanostructured systems, the significantly larger area of interface and grain boundaries produces an increase in the density of mobile defects in the space-charge region. This in turn leads to a completely different electrochemical behaviour from that of bulk polycrystalline materials[86,89]. According to Maier[88], these 'trivial' size effects, resulting simply from an increased proportion of the interface, should be distinguished from 'true' size effects occurring when the particle size is smaller than four times the Debye length, where the local properties are changed in terms of ionic and electronic charge-carrier transport. Interestingly, the same space-charge model was

used by Maier to explain the observed increase in ionic conductivity of dry or hybrid Li-based polymer systems loaded with nano-inorganic fillers (SiO_2, Al_2O_3, TiO_2) as discussed previously.

Notwithstanding the importance of nanostructured materials, the performance of practical fuel cells remains limited by scale-up, stack housing design, gas manifold and sealing. Although progress has been achieved in the direct electrochemical oxidation of alcohol and hydrocarbon fuels[62,90,91], fuel cells are still mostly fed by hydrogen. Much research is now focused on nanostructured hydrides including carbon nanotubes, nanomagnesium-based hydrides, metal-hydride/carbon nanocomposites, and alanates for hydrogen storage[92,93]. Early reports suggested hydrogen adsorption capacities of 14–20 wt% for K- and Li-doped carbon nanotubes[94,95], but today's reliable hydrogen-storage capacities in single-walled carbon nanotubes appear comparable to or even less than those of metal hydrides[96–98], and probably not sufficient to store the amount of hydrogen required for automotive applications, which has been set by the US Department of Energy as 6.5% (ref. 98). Recent developments in this field include modification of Mg-hydrides with transition metals[99,100], and the investigation of boron-nitride nanostructures[101]. Magnesium hydride, MgH_2, is often modified by high-energy ball-milling with alloying elements including[99] Ni, Cu, Ti, Nb and Al so as to obtain, after 20 h of milling, nanoparticles in the range of 20–30 nm providing hydrogen-storage capacities of about 6–11 wt% (refs 99, 100). Besides improving the hydrogen sorption kinetics of MgH_2, partial substitution of Al for Mg in Mg_2Ni hydrogen storage systems seems to increase the life-cycle characteristics, as a consequence of the existence of an Al_2O_3 film on the alloy surface[99]. Further advances resulted from the investigation of MgH_2-V nanocomposites[100] and the addition of very small amounts of nanoparticulate transition metal oxides (Nb_2O_5, WO_3, Cr_2O_3) to Mg-based hydrides[102]. The presence of vanadium as well as the particular nanostructure of the nanocomposite aids the hydrogen penetration into the material. Also, in the case of transition metal oxide promoters, the catalytic effect of compounds such as Cr_2O_3, the reactive mechanical grinding and the nanosized particles seem to produce a substantial improvement in the adsorption and desorption properties of magnesium[102].

CONCLUSION

It is a regrettable feature of important scientific discoveries that they often suffer from hyperbole; perhaps it has always been so, but the speed of today's communications exacerbates the situation. Nanoscience suffers from this disease. Yet there are many genuine scientific advances that fall under the umbrella of nanoscience. This short review demonstrates how moving from bulk materials to the nanoscale can significantly change electrode and electrolyte properties, and consequently their performance in devices for energy storage and conversion. In some cases the effects may be simple consequences of a reduction in size, for example when nanoparticulate electrodes or electrocatalysts lead to higher electrode/electrolyte contact areas and hence higher rates of electrode reaction. In others the effects may be more subtle, involving internally nanostructured materials or nanostructures with particular morphologies, for example the nanotubes. Space-charge effects at the interface between small particles can result in substantial improvements of properties. There is a profound effect of spatial confinement and contribution of surfaces, due to small particle size, on many of the properties of materials; this challenges us to develop new theory or at least adapt and develop theories that have been established for bulk materials. We also foresee that this subject will bring together the disciplines of materials chemistry and surface science, as both are necessary to understand nanomaterials.

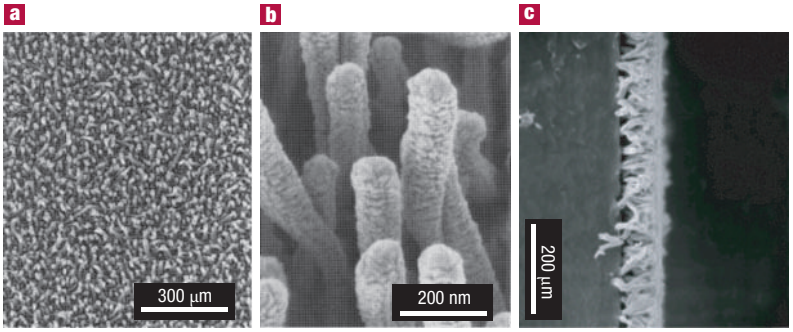

Figure 8 Platinum-coated nanostructured whisker supports (0.25 mg cm^{-2}). a, Plane view; b, 45° view (higher magnification). The nanostructured film of the MEA (**c**) shows the Pt-coated nanowhiskers sandwiched between the PEM and the gas-diffusion layer. Courtesy of R. Atanasoski, 3M, St. Paul, Minnesota, USA.

doi:10.1038/nmat1368

References

1. Nazar, L. F. *et al.* Nanostructured materials for energy storage. *Int. J. Inorg. Mater.* **3,** 191–200 (2001).
2. Hirshes, M. Nanoscale materials for energy storage. *Mater. Sci. Eng. B* **108,** 1 (2004).
3. Scrosati, B. Challenge of portable power. *Nature* **373,** 557–558 (1995).
4. Tarascon, J.-M. & Armand, M. Issues and challenges facing rechargeable batteries. *Nature* **414,** 359–367 (2001).
5. Wakihara, W. & Yamamoto, O. (eds) *Lithium Ion Batteries—Fundamentals and Performance* (Kodansha-Wiley-VCH, Weinheim, 1998).
6. van Schalkwijk, W. & Scrosati, B. (eds) *Advances in Lithium-Ion Batteries* (Kluwer Academic/Plenum, New York, 2002).
7. Huggins, R. A. in *Handbook of Battery Materials* (ed. Besenhard, J. O.) Part III, Chapter 4 (Wiley-VCH, Weinheim, 1999).
8. Winter, M. & Besenhard, J. O. Electrochemical lithiation of tin and tin-based intermetallic and composites. *Electrochim. Acta* **45,** 31–50 (1999).
9. Nazar, L. F. & Crosnier, O. In *Lithium Batteries Science and Technology* (eds Nazri,G.-A. & Pistoia, G.) 112–143 (Kluwer Academic/Plenum, Boston, 2004).
10. Idota, Y., Kabuto, T., Matsufuji, A., Maekawa, Y. & Miyasaki, T. Tin-based amorphous oxides: a high-capacity lithium-ion storage material. *Science* **276,** 1395–1397 (1997).
11. Mao, O. & Dahn,J. R. Mechanically alloyed Sn–Fe(–C) powders as anode materials for Li ion batteries. III. Sn_2Fe:$SnFe_3C$ active/inactive composites. *J. Electrochem. Soc.* **146,** 423–427 (1999).
12. Beaulieu, L. Y. & Dahn, J. R. The reaction of lithium with Sn–Mn–C intermetallics prepared by mechanical alloying. *J. Electrochem. Soc.* **147,** 3237–3241(2000).
13. Graetz, J., Ahn, C. C., Yazami, R. & Fuetz, B. Highly reversible lithium storage in nanostructured silicon. *Electrochem. Solid-State Lett.* **6**, A194–197 (2003).
14. Yang, J. *et al.* Si/C composites for high capacity lithium storage materials. *Electrochem. Solid-State Lett.* **6**, A154–156 (2003).
15. Novak, P. *et al.* in *Int. Meeting Li Batteries IMLB12 Nara, Japan* Abstract 9 (2004).
16. Ikeda, H. *et al.* in *Proc. 42nd Battery Symposium, Yokohama, Japan* 282 (2001).
17. Green, M., Fielder, E., Scrosati, B., Wachtler, M. & Serra Moreno, J. Structured silicon anodes for lithium battery applications. *Electrochem. Solid-State Lett.* **6**, A75–79 (2003).
18. Armstrong, A. R., Armstrong, G., Canales, Garcia, J. R. &Bruce, P. G. Lithium intercalation intoTiO_2-B nanowires. *Adv. Mater.* (in the press).
19. Poizot, P., Laruelle, S., Grugeon, S., Dupont, L. & Tarascon, J.-M. Nano-sized

transition metal oxides as negative electrode material for lithium-ion batteries. *Nature* **407,** 496–499 (2000).
20. Tarascon, J.-M., Grugeon, S., Laruelle, S., Larcher, D. & Poizot, P. In *Lithium Batteries Science and Technology* (eds Nazri, G.-A. & Pistoia, G.) Ch. 7, 220–246 (Kluwer Academic/Plenum, Boston, 2004).
21. Denis, S., Baudrin, E., Touboul, M. & Tarascon, J.-M. Synthesis and electrochemical properties vs. Li of amorphous vanadates of general formula RVO_4 (R = In, Cr, Fe, Al, Y) *J. Electrochem. Soc.* **144,** 4099–4109 (1997).
22. Leroux, F., Coward, G. R., Power, W. P. & Nazar, L. F. Understanding the nature of low-potential Li uptake into high volumetric capacity molybedenum oxides. *Electrochem Solid-State Lett.* **1,** 255–258 (1998).
23. Balaya, P., Li, H., Kienle, L. & Maier, J. Fully reversible homogeneous Li storage in RuO_2 with high capacity. *Adv. Funct. Mater.* **13,** 621–625 (2003).
24. Badway, F., Cosandey, F., Pereira, N. & Amatucci, G. G. Carbon metal fluoride nanocomposites: high capacity reversible metal fluoride conversion materials as rechargeable positive electrodes for Li batteries. *J. Electrochem. Soc.* **150**, A1318–1327 (2003).
25. Li, H., Ritcher, G. & Maier, J. Reversibile formation and decomposition of LiF clusters using transition metal fluorides as precursors and their application in rechargeable Li batteries. *Adv. Mater.* **15,** 736–739 (2003).
26. Jamnik, J, & Maier, J. Nanocrystallinity effects in lithium battery materials. Aspects of nano-ionics. Part IV. *Phys. Chem. Chem. Phys.* **5,** 5215–5220 (2003).
27. Larcher, D. *et al.* Effect of particle size on lithium intercalation into α-Fe_2O_3. *J. Electrochem. Soc.* **150**, A133–139 (2003).
28. Sides, C. R., Li, N. C., Patrissi, C. J., Scrosati, B. & Martin, C. R. Nanoscale materials for lithium-ion batteries. *Mater. Res. Bull.* **27,** 604–607 (2002).
29. Nordliner, S., Edström, K. & Gustafsson, T. Electrochemistry of vanadium oxide nanotubes. *Electrochem. Solid State Lett.* **4**, A129 (2001).
30. Le, D. B. *et al.* High surface area V_2O_5 aerogel intercalation electrodes. *J. Electrochem. Soc.* **143,** 2099–2104 (1996).
31. Dong, W., Rolison, D. R. & Dunn, B. Electrochemical properties of high surface area vanadium oxides aerogels. *Electrochem. Solid State Lett.* **3,** 457–459 (2000).
32. Thackeray, M. M., David, W. I. F., Bruce, P. G. & Goodenough, J. B. Lithium insertion into manganese spinels. *Mater. Res. Bull.* **18,** 461–472 (1983).
33. Robertson, A. D., Armstrong, A. R. & Bruce, P. G. Layered $Li_xMn_yCo_{1-y}O_2$ intercalation electrodes: influence of ion exchange on capacity and structure upon cycling. *Chem. Mater.* **13**, 2380–2386 (2001).
34. Shao-Horn, Y. *et al.* Structural characterisation of layered $LiMnO_2$ electrodes by electron diffraction and lattice imaging. *J. Electrochem. Soc.* **146,** 2404–2412 (1999).
35. Wang, H. F., Jang, Y. I. & Chiang, Y.-M. Origin of cycling stability in monoclinic and orthorhombic-phase lithium manganese oxide cathodes. *Electrochem. Solid-State Lett.* **2,** 490–493 (1999).
36. Kang, S. H., Goodenough, J. B. & Rabenberg, L. K. Effect of ball-milling on 3 V capacity of lithium manganese oxospinel cathodes. *Chem. Mater.* **13**, 1758–1764 (2001).
37. Reed, J., Ceder, G. & van der Ven, A. Layered-to-spinel phase transformation in Li_xMnO_2. *Electrochem. Solid-State Lett.* **4**, A78–81 (2001).
38. Padhi, A. K., Nanjundaswamy, K. S., Masquelier, C., Okada, S. & Goodenough, J. B. Effect of structure on the Fe^{3+}/Fe^{2+} redox couple in iron phosphates. *J. Electrochem. Soc.* **144,** 1609–1613 (1997).
39. Ravet, A. *et al.* Electroactivity of natural and synthetic triphylite. *J. Power Sources* **97–98,** 503–507 (2001).
40. Huang, H., Yin, S.-C. & Nazar, L. F. Approaching theoretical capacity of $LiFePO_4$ at room temperature and high rates. *Electrochem. Solid-State Lett.* **4,** A170–172 (2001).
41. Croce, F., Scrosati, B., Sides, B. R. & Martin, C. R. in *206th Meeting Electrochemical Society, Honolulu, Hawaii* Abstract 241(2004).
42. Scrosati. B. & Vincent, C. A. Polymer electrolytes: the key to lithium polymer batteries. *Mater. Res. Soc. Bull.* **25,** 28–30 (2000).
43. Croce, F., Appetecchi, G. B., Persi, L. & Scrosati, B. Nanocomposite polymer electrolytes for lithium batteries. *Nature* **394,** 456–458 (1998).
44. MacFarlane, D. R., Newman, P. J., Nairn, K. M. & Forsyth, M. Lithium-ion conducting ceramic/polyether composites. *Electrochim. Acta* **43,** 1333–1337 (1998).
45. Kumar, B., Rodrigues, S. J. & Scanlon, L. Ionic conductivity of polymer–ceramic composites. *J. Electrochem. Soc.* **148**, A1191–1195 (2001).
46. Maier, J. Ionic conduction in space charge regions. *Prog. Solid State Chem.* **23,** 171–263 (1995).
47. Appetecchi, G. B., Croce, F., Persi, L., Ronci, F. & Scrosati, B. Transport and interfacial properties of composite polymer electrolytes. *Electrochim. Acta* **45,** 1481–1490 (2000).
48. Angell, C. A., Liu, C. & Sanchez, S. Rubbery solid electrolytes with dominant cationic transport and high ambient conductivity. *Nature* **362,** 137–139(1993).
49. Hawett, P. C., MacFarlane, D. R. & Hollenkamp, A. F. High lithium metal cycling efficiency in a room-temperature ionic liquid. *Electrochem. Solid-State Lett.* **7**, A97–101 (2004).
50. MacGlashan, G., Andreev, Y. G. &. Bruce, P. G. The structure of poly(ethylene oxide)$_6$:$LiAsF_6$. *Nature* **398,** 792–794 (1999).
51. Gadjourova, Z., Andreev, Y. G., Tunstall D. P. & Bruce, P. G. Ionic conductivity in crystalline polymer electrolytes. *Nature* **412,** 520–523 (2001).
52. Stoeva, Z., Martin-Litas, I., Staunton, E., Andreev Y. G. & Bruce, P. G. Ionic conductivity in the crystalline polymer electrolytes PEO_6:$LiXF_6$, *X* = P, As, Sb. *J. Am. Chem. Soc.* **125,** 4619–2626 (2003).
53. Christie, A. M., Lilley, S. J., Staunton, E, Andreev, Y. G. & Bruce, P. G. Increasing the conductivity of crystalline polymer electrolytes. *Nature* **433,** 50–53 (2005).
54. Conway, B. E. *Electrochemical Supercapacitors.* (Kluwer Academic/Plenum, New York, 1999).
55. Mastragostino, M., Arbizzani, C. & Soavi, F. In *Advances in Lithium-Ion Batteries.* (Van Schalkwijk, W. & Scrosati, B., eds) Ch. 16, 481–505 (Kluwer Academic/Plenum, New York, 2002).
56. Arbizzani, C., Mastragostino, M. & Soavi, S. New trends in electrochemical supercapacitors. *J. Power Sources* **100,** 164–170 (2001).
57. Wang, J. *et al.* Morphological effects on the electrical and electrochemical properties of carbon aerogels. *J. Electrochem. Soc.* **148,** D75–77 (2001).
58. Niu, C., Sichjel, E. K., Hoch, R., Hoi, D. & Tennent, H. High power electrochemical capacitors based on carbon nanotube electrodes. *Appl. Phys. Lett.* **70,** 1480–1482 (1997).
59. Nelson, P. A. & Owen, J. R. A high-performance supercapacitor/battery hybrid incorporating templated mesoporous electrodes. *J. Electrochem. Soc.* **150,** A1313–1317 (2003).
60. Amatucci, G. G., Badway, F., Du Pasquier, A. & Zheng, T. An asymmetric hybrid nonaqueous energy storage cell. *J. Electrochem. Soc.* **148,** A930–939 (2001).
61. Brodd, R. J. *et al.* Batteries 1977 to 2002. *J. Electrochem. Soc.* **151**, K1–11 (2004).
62. Srinivasan, S., Mosdale, R., Stevens, P. & Yang, C. Fuel cells: reaching the era of clean and efficient power generation in the twenty-first century. *Annu. Rev. Energy Environ.* **24,** 281–238 (1999).
63. Giordano, N. *et al.* Analysis of platinum particle size and oxygen reduction in phosphoric acid. *Electrochim. Acta* **36,** 1979–1984 (1991).
64. Freund, A., Lang, J., Lehman, T. & Starz, K. A. Improved Pt alloy catalysts for fuel cells. *Catal. Today* **27,** 279–283 (1996).
65. Mukerjee, S., Srinivasan, S., Soriaga, M. P. & McBreen, J. Role of structural and electronic properties of Pt and Pt alloys on electrocatalysis of oxygen reduction. An *in-situ* XANES and EXAFS investigation. *J. Electrochem. Soc.* **142,** 1409–1422 (1995).
66. Aricò, A. S., Srinivasan, S. & Antonucci, V. DMFCs: From fundamental aspects to technology development. *Fuel Cells* **1,** 133–161 (2001).
67. Schmidt, T. J. *et al.* Electrocatalytic activity of Pt–Ru alloy colloids for CO and CO/H_2 electrooxidation: stripping voltammetry and rotating-disk measurements. *Langmuir* **14,** 2591–2595 (1997).
68. Chrzanowski, W. & Wieckowski, A. Enhancement in methanol oxidation by spontaneously deposited ruthenium on low-index platinum-electrodes. *Catal. Lett.* **50,** 69–75 (1998).
69. Brankovic, S. R., Wang, J. X. & Adzic, R. R. Pt submonolayers on Ru nanoparticles–a novel low Pt loading, high CO tolerance fuel-cell electrocatalyst. *Electrochem. Solid-State Lett.* **4**, A217–220 (2001).
70. Hockaday, R. G. *et al.* in *Proc. Fuel Cell Seminar, Portland, Oregon, USA* 791–794 (Courtesy Associates, Washington DC, 2000).
71. Sun, G. R., Wang, J. T.& Savinell, R. F. Iron(III) tetramethoxyphenylporphyrin (Fetmpp) as methanol tolerant electrocatalyst for oxygen reduction in direct methanol fuel-cells. *J. Appl. Electrochem.* **28,** 1087–1093 (1998).
72. Reeve, R. W., Christensen, P. A., Hamnett, A., Haydock, S. A. & Roy, S. C. Methanol tolerant oxygen reduction catalysts based on transition metal sulfides. *J. Electrochem. Soc.* **145,** 3463–3471 (1998).
73. Nolte, R., Ledjeff, K., Bauer, M. & Mulhaupt, R. Partially sulfonated poly(arylene ether sulfone)—a versatile proton conducting membrane material for modern energy conversion technologies. *J. Membrane Sci.* **83,** 211–220 (1993).
74. Kerres, J., Ullrich, A., Meier, F. & Haring, T. Synthesis and characterization of novel acid-base polymer blends for application in membrane fuel cells. *Solid State Ionics* **125,** 243–249 (1999).
75. Alberti, G. & Casciola, M. Composite membranes for medium-temperature PEM fuel cells. *Annu. Rev. Mater. Res.* **33,** 129–154 (2003).
76. Savadogo, O. Emerging membranes for electrochemical systems: (I) solid polymer electrolyte membranes for fuel cell systems. *J. New Mater. Electrochem. Syst.* **1,** 47–66 (1998).
77. Li, Q., He, R., Jensen, J. O. & Bjerrum, N. J. Approaches and recent development of polymer electrolyte membranes for fuel cells operating above 100 °C. *Chem. Mater.* **15,** 4896–4815 (2003).
78. Kreuer, K. D. On the development of proton conducting polymer membranes for hydrogen and methanol fuel cells. *J. Membrane Sci.* **185,** 29–39 (2001).
79. Watanabe, M., Uchida, H., Seki, Y., Emori, M. & Stonehart, P. Self-humidifying polymer electrolyte membranes for fuel cells. *J. Electrochem. Soc.* **143,** 3847–3852 (1996).
80. Aricò, A. S., Creti, P., Antonucci, P. L. & Antonucci, V. Comparison of ethanol and methanol oxidation in a liquid feed solid polymer electrolyte fuel cells at high temperature. *Electrochem. Solid-State Lett.* **1,** 66–68 (1998).
81. Aricò, A. S., Baglio, V., Di Blasi, A. & Antonucci, V. FTIR spectroscopic investigation of inorganic fillers for composite DMFC membranes. *Electrochem. Commun.* **5,** 862–866 (2003).
82. Kreuer, K. D., Paddison, S. J., Spohr, E. & Schuster, M. Transport in proton conductors for fuel cell applications: simulation, elementary reactions and phenomenology. **104,** 4637–4678 (2004).

83. Kreuer, K. D. On the development of proton conducting materials for technological applications. *Solid State Ionics* **97,** 1–15 (1997).
84. Debe, M. K. *Handbook of Fuel Cells—Fundamentals, Technology and Applications* Vol. 3 (eds Vielstich, W., Gasteiger, H. A. & Lamm, A.) Ch. 45, 576–589 (Wiley, Chichester, UK, 2003).
85. Atanasoski, R. in *4th Int. Conf. Applications of Conducting Polymers, ICCP-4, Como, Italy* Abstract 22 (2004).
86. Schoonman, J. Nanoionics. *Solid State Ionics* **157,** 319–326 (2003).
87. Steele, B. C. H. Current status of intermediate temperature fuel cells (It-SOFCs). *European Fuel Cell News* **7,** 16–19 (2000).
88. Maier, J. Defect chemistry and ion transport in nanostructured materials. Part II Aspects of nanoionics. *Solid State Ionics* **157,** 327–334 (2003).
89. Knauth, P & Tuller, H. L. Solid-state ionics: roots, status, and future-prospects. *J. Am. Ceram. Soc.* **85,** 1654–1680 (2002).
90. Perry Murray, E., Tsai, T.& Barnett, S. A. A direct-methane fuel cell with a ceria-based anode. *Nature* **400,** 649–651 (1999).
91. Park, S., Vohs, J. M. & Gorte, R. J. Direct oxidation of hydrocarbons in a solid-oxide fuel cell. *Nature* **404,** 265–267 (2000).
92. Zhou, Y. P., Feng, K., Sun, Y. & Zhou, L. A brief review on the study of hydrogen storage in terms of carbon nanotubes. *Prog. Chem.* **15,** 345–350 (2003).
93. Schlappach, L. & Zuttel, A. Hydrogen-storage materials for mobile applications. *Nature* **414,** 353–358 (2001).
94. Dillon A. C. *et al.* Storage of hydrogen in single-walled carbon nanotubes. *Nature* **386,** 377–379 (1997).
95. Chambers, A., Park, C., Baker, R. T. K. & Rodriguez, N. M. Hydrogen storage in graphite nanofibers. *J. Phys. Chem.* **102,** 4253–4256 (1998).
96. Yang, R. T. Hydrogen storage by alkali-doped carbon nanotubes—revisited. *Carbon* **38,** 623–626 (2000).
97. Dillon, A. C.& Heben, M. J. Hydrogen Storage using carbon adsorbents—past, present and future. *Appl. Phys. A* **72,** 133–142 (2001).
98. Hirscher, M. & Becher, M. Hydrogen storage in carbon nanotubes. *J. Nanosci. Nanotechnol.* **3,** 3–17 (2003).
99. Shang, C. X., Bououdina, M., Song, Y. & Guo, Z. X. Mechanical alloying and electronic simulation of MgH_2–M systems (M–Al, Ti, Fe, Ni, Cu, and Nb) for hydrogen storage. *Int. J. Hydrogen Energy* **29,** 73–80 (2004).
100. Bobet, J. L., Grigorova, E., Khrussanova, M., Khristov, M. & Peshev, P. Hydrogen sorption properties of the nanocomposite 90wt.% Mg_2Ni–10 wt.% V. *J. Alloys Compounds* **356,** 593–597 (2003).
101. Ma, R. Z. *et al.* Synthesis of boron-nitride nanofibers and measurement of their hydrogen uptake capacity. *Appl. Phys. Lett.* **81,** 5225–5227 (2002).
102. Bobet, J. L., Desmoulinskrawiec, S., Grigorova, E., Cansell, F. & Chevalier, B. Addition of nanosized Cr_2O_3 to magnesium for improvement of the hydrogen sorption properties. *J. Alloys Compounds* **351,** 217–221 (2003).
103. Audemer, A., Wurm, C., Morcrette, M., Gwizdala, S. & Masquellier, C. Carbon-coated metal bearing powders and process for production thereof. World Patent WO 04/001881 A2 (2004).

Acknowledgements

We thank M. Mastragostino of the university of Bologna for suggestions and help in completing the supercapacitors part of this review. Support from the European Network of Excellence 'ALISTORE' network is acknowledged. P.G.B. is indebted to the Royal Society for financial support.
Correspondence should be addressed to B.S.

Competing financial interests

The authors declare that they have no competing financial interests.